

Supporting Information

Effect of shell thickness and composition on blinking suppression and the blinking mechanism in 'giant' CdSe/CdS nanocrystal quantum dots

Javier Vela,¹ Han Htoon,² Yongfen Chen,³ Young-Shin Park,² Yagnaseni Ghosh,² Peter M. Goodwin,⁴ James H. Werner,⁴ Nathan P. Wells,⁵ Joanna L. Casson,² Jennifer A. Hollingsworth^{*2}

¹ Department of Chemistry, Iowa State University, Ames, IA 50011

² Chemistry Division and the Center for Integrated Nanotechnologies, Los Alamos National Laboratory, Los Alamos, New Mexico 87545

³ Life Technologies, Eugene, Oregon 97402

⁴ Materials Physics and Applications Division, Center for Integrated Nanotechnologies, Los Alamos National Laboratory, Los Alamos, NM 87545

⁵ LIDAR and Atomic Clocks, Photonics Technology Department, Aerospace Corporation, El Segundo, CA 90245

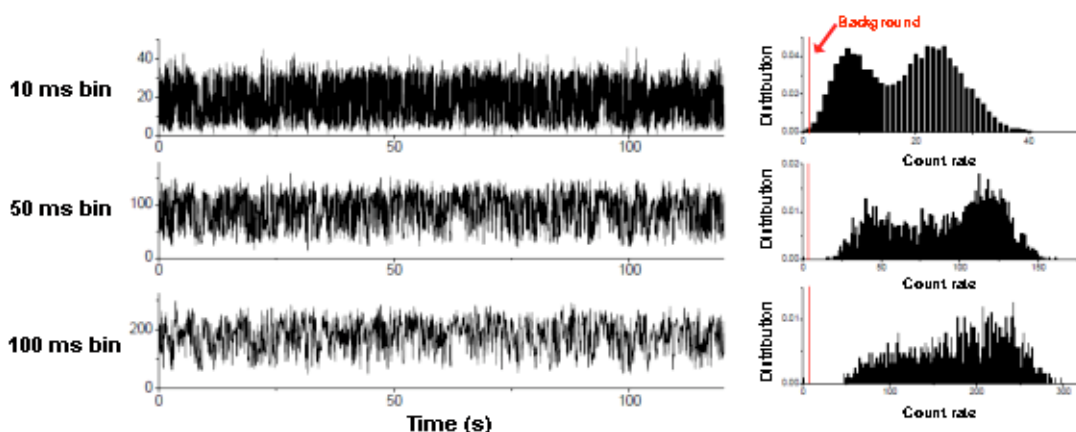


Figure S1. PL intensity time traces (left) and count-rate distributions (right) of a CdSe/12CdS g-NQD sample at different time binnings measured by a time-correlated single-photon-counting approach. The measurements show that although the g-NQD PL intensity is fluctuating widely, and showing two distributions of count rates (bimodal), the intensity levels do not drop to completely ‘off’ (dark) states. These data suggest that the “off level” which is arbitrarily set in CCD-based measurements may correspond, instead, to a lower-count-rate state.

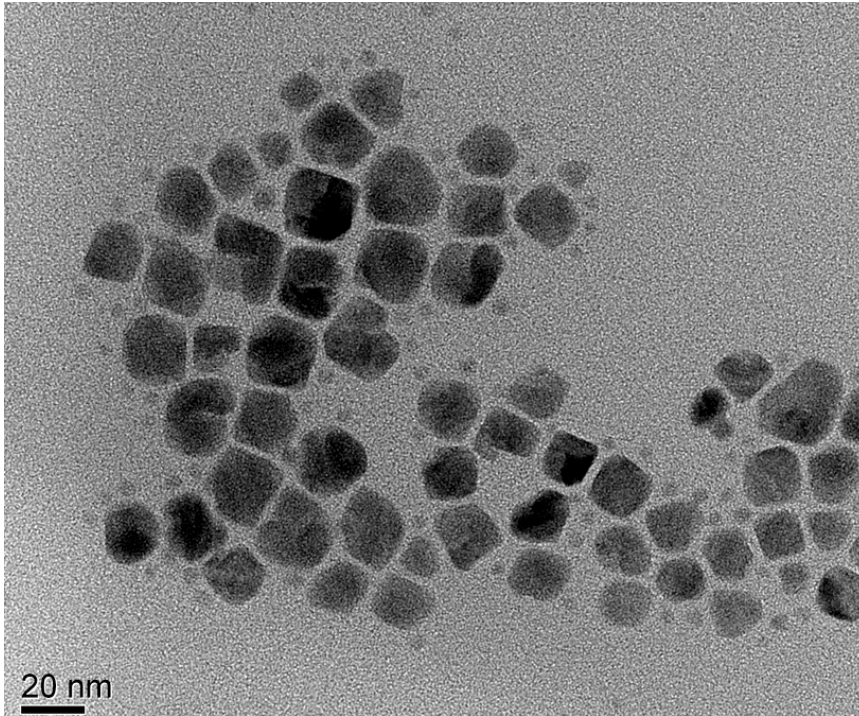


Figure S2. TEM image of a 'crude' (non-size-selected) CdSe/18CdS sample showing the bimodal size distribution that sometimes results from SILAR synthesis of ultra-thick-shell CdSe/CdS core/shell g-NQDs.

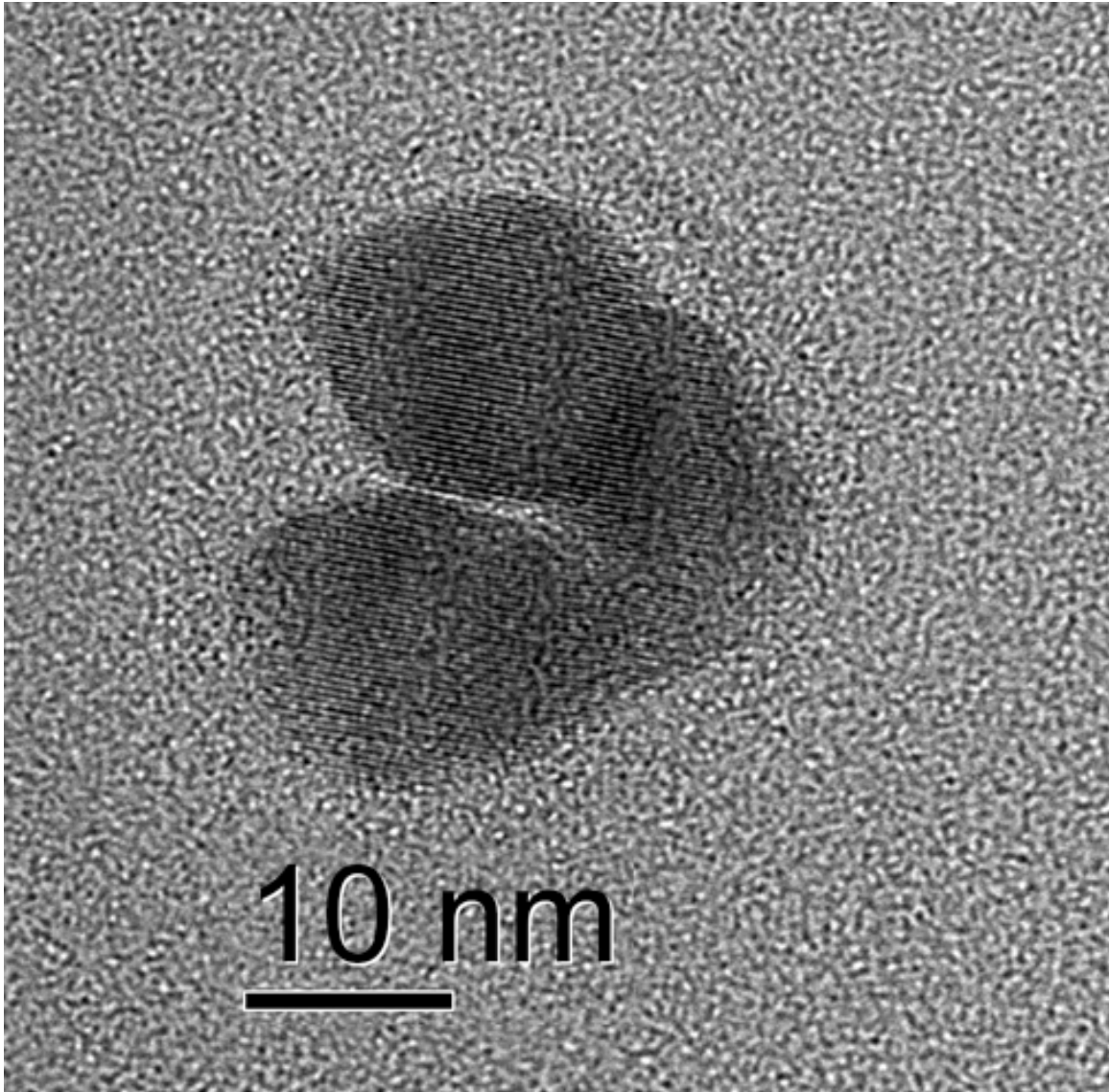


Figure S3. High-resolution TEM image of a defective ‘heart-shaped’ g-NQD found in a CdSe/19CdS sample. This unusual shape is fairly common among the defective ultra-thick-shell sub-populations.

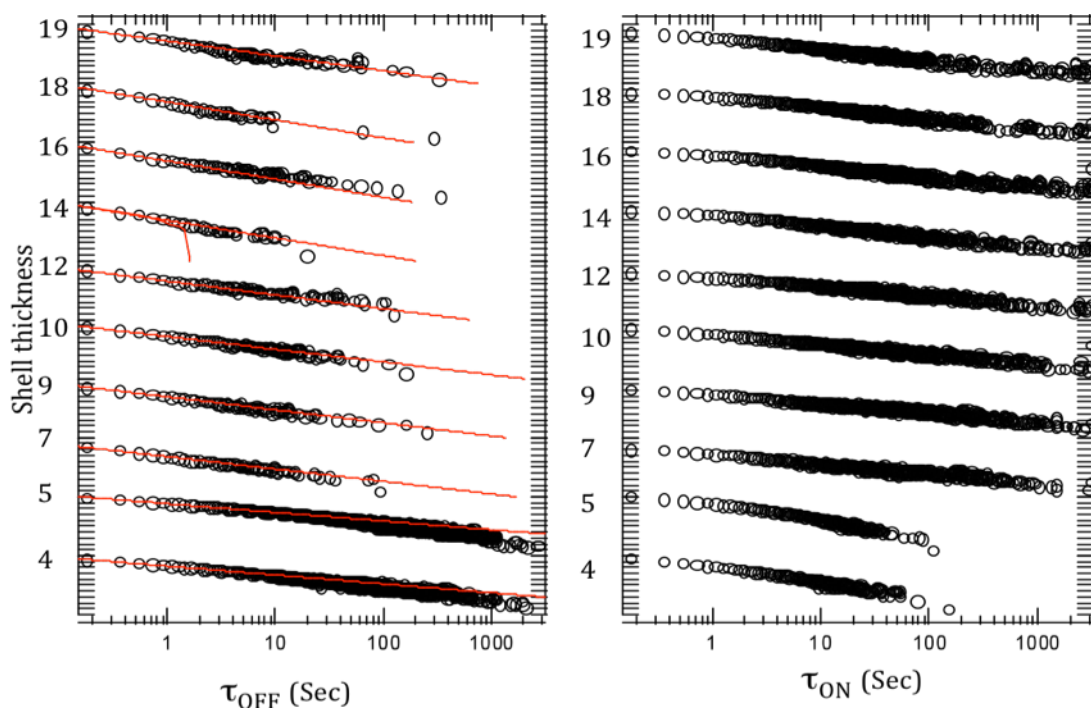


Figure S4. $P(\tau_{off})$ and $P(\tau_{on})$ of g-NQDs possessing different shell thicknesses. The lowest two curves for the shell thicknesses of 4 and 5 shells are extracted from the whole ensemble of NQDs, while the remaining curves are extracted from the sub-ensemble with total on-time fraction $>75\%$.

Further verification of the single-NQD nature of the samples used to assess blinking behavior. Our assessments of on-time fractions were independent of sample concentration (Table S1) when otherwise identical samples were analyzed consecutively and in an equivalent manner (i.e., instrument conditions reproducible and operator adhering to identical data analysis protocol). In contrast, if NQDs had tended to aggregate, blinking statistics would have been expected to trend with sample concentration, as the extent of NQD aggregation would have changed as a function of dilution.

Table S1.

Sample (core/shell NQDs)	Number of NQDs observed in the 40 x 40 μm data collection area	On-Time fraction $\geq 80\%$
CdSe/10CdS	54	43 %
CdSe/10CdS	304	45 %
CdSe/19CdS	85	62 %
CdSe/19CdS	315	57 %